Cellular Physiology and Biochemistry

Cell Physiol Biochem 2018;49:2163-2173
DOI: 10.1159/000493819
Published online: 27 September 2018
Accepted: 18 September 2018

Original Paper

Omi/HtrA2 Regulates a Mitochondria-Dependent Apoptotic Pathway in a Murine Model of Septic Encephalopathy

Pengfei Wang[a] Yueyu Hu[b] Danhua Yao[a] Yousheng Li[a]

[a]Department of General Surgery, Shanghai Ninth People's Hospital, Shanghai Jiaotong University School of Medicine, Shanghai, [b]Department of Neurology, the Fourth People's Hospital Affiliated to Tongji University, Shanghai, China

Key Words
Sepsis-associated encephalopathy • Apoptosis • CLP • UCF-101 • Omi/HtrA2

Abstract
Background/Aims: the pathogenesis of sepsis-associated encephalopathy (SAE) is multifactorial, involving neurotransmitter alterations, inflammatory cytokines, oxidative damage, mitochondrial dysfunction, apoptosis, and other factors. Mitochondria are major producers of reactive oxygen species, resulting in cellular injury. Omi/HtrA2 is a proapoptotic mitochondrial serine protease involved in caspase-dependent cell death; it is translocated from mitochondria to the cytosol after an apoptotic insult. We previously found that UCF-101, a specific inhibitor of Omi/HtrA2, has neuroprotective effects on cerebral oxidative injury and cognitive impairment in septic rats. In this study, the mechanisms and molecular pathways underlying these effects were investigated. ***Methods:*** Male Sprague–Dawley rats were subjected to cecal ligation and puncture (CLP) or sham-operated laparotomy and were administered vehicle or UCF-101 (10 μmol/kg). The hippocampus was isolated for subsequent analysis. Omi/HtrA2 expression in the mitochondria or cytosol was evaluated by immunofluorescence or western blotting. Terminal deoxynucleotidyl transferase dUTP nick end labeling staining was utilized to evaluate levels of apoptosis, and western blotting was used to evaluate apoptosis-related proteins, such as cleaved caspase-3, caspase-9, and poly (ADP-ribose) polymerase (PARP). Tight junction expression was assessed by immunofluorescence and western blotting. Mitochondrial function, inflammatory cytokines, and oxidative stress were also assayed. In addition, a wet/dry method was used to evaluate brain edema and Evans blue extravasation was used to evaluate blood–brain barrier (BBB) integrity. ***Results:*** After CLP treatment, the hippocampus exhibited a mild increase in Omi/HtrA2 expression; cytosolic Omi/HtrA2 expression increased significantly, whereas mitochondrial Omi/HtrA2 expression was reduced, indicating that CLP-induced oxidative stress resulted in the translocation of Omi/HtrA2 from mitochondria to the cytosol. Hippocampal cleaved caspase-3, caspase-9, and PARP levels were significantly higher in animals treated with CLP than in sham-operated

Yueyu Hu
and Yousheng Li

Department of Neurology, the Fourth People's Hospital to Tongji University, Shanghai;
Department of General Surgery, Shanghai Ninth People's Hospital, Shanghai Jiaotong
University School of Medicine, Shanghai (China); E-Mail huyueyu2008@163.com; liys@medmail.com.cn

animals, while XIAP expression was lower. Treatment with UCF-101 prevented the mobilization of Omi/HtrA2 from mitochondria to the cytosol, attenuated XIAP degradation, and decreased cleaved caspase-3, caspase-9, and PARP expression as well as apoptosis. UCF-101 also reversed the decreased mitochondrial complex I, II, and III respiration and the reduced ATP caused by CLP. In addition, UCF-101 treatment resulted in a significant improvement in BBB integrity, as demonstrated by increased occludin, claudin-5, and zonula occludens 1 levels and reduced Evans blue extravasation. No significant effects of UCF-101 on brain edema were found. Inflammatory cytokines and oxidative stress were significantly higher in the CLP-treated group than in the sham-operated group. However, the inhibition of Omi/HtrA2 by UCF-101 significantly alleviated these responses. ***Conclusion:*** Our data indicated that Omi/HtrA2 regulates a mitochondria-dependent apoptotic pathway in a murine model of septic encephalopathy. Inhibition of Omi/HtrA2 by UCF-101 leads to neuroprotection by inhibiting the cytosolic translocation of Omi/HtrA2 and antagonizing the caspase-dependent apoptosis pathway. Therapeutic interventions that inhibit Omi/HtrA2 translocation or protease activity may provide a novel method to treat SAE.

Introduction

Sepsis-associated encephalopathy (SAE), which is associated with cognitive disorders, is a frequent and severe neurological manifestation of sepsis [1]. It is clinically characterized by changes in either mental status ranging from delirium to coma or motor activity ranging from agitation to hypoactivity. Alterations in alertness and consciousness are independent factors related to prognosis, and patients often require long-term medical interventions to support functional recovery after SAE development [2]. The high incidence of SAE emphasizes the importance of the early detection and treatment of sepsis-associated brain dysfunction.

The pathogenesis of SAE is multifactorial, involving neurotransmitter alterations, inflammatory cytokines, oxidative damage, mitochondrial dysfunction, apoptosis, and so on. Oxidative damage due to an imbalance between the generation and elimination of reactive oxygen species (ROS) is a major cause of brain damage in SAE [1, 3]. Accordingly, oxidative stress may promote the pathogenesis of SAE by enhancing the expression of proinflammatory cytokines, promoting apoptosis, and/or interfering with blood–brain barrier (BBB) function [4, 5]. Mitochondria re major producers of ROS, resulting in injury [6].

Omi/HtrA2 is a proapoptotic mitochondrial serine protease involved in caspase-dependent and caspase-independent cell apoptosis [7, 8]. UCF-101 is a specific inhibitor of Omi/HtrA2; we previously demonstrated that UCF-101 has neuroprotective effects on cerebral oxidative injury and cognitive impairment in septic rats [9]. However, the molecular pathways underlying these effects have not been investigated.

Materials and Methods

Reagents

The following antibodies were used: rabbit anti-zonula occludens 1 (ZO-1), anti-cleaved-caspase-3, anti-cleaved-caspase-9, anti-poly (ADP-ribose) polymerase (PARP), and goat anti-rabbit conjugated to Alexa Fluor 488 and 594 from Cell Signaling Technology (Danvers, MA); rabbit anti-claudin 5 and occludin from Invitrogen (Eugene, OR); and rabbit anti-Omi/HtrA2, anti-mitofusin 2 (Mfn2), and dynamin-related protein 1 (Drp1) from Santa Cruz Biotechnology (Santa Cruz, CA). Other secondary antibodies were purchased from Dianova (Barcelona, Spain) and Invitrogen. UCF-101 was purchased from Calbiochem (Darmstadt, Germany). Other molecular biology grade chemicals were obtained from Sigma-Aldrich (St. Louis, MO) or Bio-Rad Laboratories (Hercules, CA).

Animals and UCF-101 preparation

Male Sprague–Dawley rats, weighing 150 to 200 g, were used after a 5- to 7-day acclimatization period. Animals were housed in individual cages in a 12:12-h light:dark temperature-controlled environment and were fasted for 8 h but allowed water ad libitum before the experiments. All procedures were performed in accordance with "Principles of Laboratory Animal Care" (NIH publication No. 85-23, revised 1985).

UCF-101 (Calbiochem) was dissolved in dimethyl sulfoxide and diluted in 5% glucose solution to 10 μmol/kg for intraperitoneal administration. Thirty minutes prior to cecal ligation and puncture (CLP) model establishment, animals were administered vehicle or UCF-101 (10 μmol/kg).

Experimental protocol

The CLP model was constructed as previously described [9]. Animals were anesthetized with pentobarbital (30 mg/kg, intraperitoneally). In brief, under sterile surgical conditions, a 2-cm abdominal incision was made along the ventral surface of the abdomen to expose the cecum, which was then ligated below the ileocecal junction with no bowel obstruction. The cecum was punctured once with an 18-gauge needle, and the fecal contents were allowed to leak into the peritoneum by gently squeezing the cecum. The bowel was then returned to the abdomen and the abdominal cavity was closed. The sham-operated rats were subjected to laparotomy, and the cecum was manipulated but neither ligated nor punctured. All rats that underwent surgical manipulation received a subcutaneous injection of saline solution (3 mL/100 g body weight) plus antibiotics (ceftriaxone at 30 mg/kg) every 6 h for resuscitation.

The animals were categorized into four groups: (1) sham plus normal saline (10 mL/kg), (2) sham plus UCF-101 (10 μmol/kg), (3) CLP plus normal saline (10 mL/kg), and (4) CLP plus UCF-101 (10 μmol/kg). After 24 h, animals were sacrificed. Their brains were harvested and the hippocampus was quickly isolated by hand dissection using a magnifying glass and a thin brush; the dissection was based on histological distinctions described by Paxinos and Watson [10]. Samples were stored at -80°C for subsequent analysis.

Assessment of BBB integrity

A modified Evans blue extravasation method was used to evaluate BBB integrity [11] . Briefly, pre-prepared warm 2% Evans blue dye was infused into the femoral vein after 22 h post-CLP. After 2 h, the rats were perfused with normal saline to wash residual dye from the blood vessels. The infiltrated Evans blue dye in the right and left hemispheres was quantified using a spectrophotometer at 610 nm. The dye in the cerebellum was used as an internal control. The content of the dye was calibrated with a standard curve of known dyes.

Brain edema (BE) assay

A common wet/dry method was used to evaluate BE [12]. The brain hemispheres were immediately weighed to obtain the wet weight and dried in a 100°C oven for 24 h to obtain the dry weight. The water content was calculated by the following formula: water content (wet weight %) = [(wet weight) − (dry weight)]/(wet weight) × 100%.

Apoptosis assay

The terminal deoxynucleotidyl transferase dUTP nick end labeling (TUNEL) assay was used to detect fragmented DNA in situ on cryosections using a commercially available test kit (ApopTag plus Peroxidase in Situ Apoptosis Detection Kit; Intergen Co., Purchase, NY) following the manufacturer's instructions. Briefly, 10 mL of the terminal deoxynucleotidyl transferase reaction mixture was added to the slides and the slides were incubated at 37°C for 90 min. The slides were washed with phosphate-buffered saline (PBS) three times and then mounted with Gelvatol (Monsanto, St. Louis, MO) and cover slipped. TUNEL-positive cells were counted using image analysis software (Image-Pro Plus 6.0) under identical conditions.

Immunofluorescence

Briefly, the slides were fixed with 10% buffered formalin, permeabilized with 0.2% Triton X-100, and subsequently blocked with 5% goat serum in PBS at room temperature for 30 min, followed by incubation with primary antibodies (1:100 to 1:150) overnight at 4°C. Then, slides were incubated for 2 h at room temperature with Alexa Fluor 488-conjugated secondary antibodies (1:800 to 1:1000). Slides were rinsed with PBS and mounted with 4',6-diamidino-2-phenylindole. Images were captured using an inverted

fluorescence microscope. Slides incubated with secondary antibodies without prior primary antibody staining served as negative controls. For mitochondrial staining, slides were incubated in 500 nM Mito Tracker Mitochondrion-Selective Probes (Invitrogen) at 37°C for 30 min.

Western blot analysis

Western blotting was performed following previously described methods [13]. Briefly, tissues were harvested and total proteins were extracted using RIPA Extraction Reagents (ProMab Biotechnology, Los Angeles, CA). Additionally, the mitochondrial and cytosolic fractions were prepared according to the manufacturer's protocol. Then, protein content in cell lysates was determined by a bicinchoninic acid (BCA) assay and equal amounts of denatured protein were subjected to sodium dodecyl sulfate polyacrylamide gel electrophoresis (5–12% acrylamide denaturing gel). Bands were electrotransferred to polyvinylidene fluoride membranes for 90 min at 220 mA (or 30 V, overnight transfer), blocked, and incubated with primary antibodies overnight (dilution range: 1:1000–1:500) in blocking buffer. Blots were washed and incubated with horseradish peroxidase-conjugated secondary antibody (1:10000) for 2 h at room temperature. The immunoreactive proteins on the membrane were visualized using an enhanced chemiluminescent detection system (Pierce, Rockford, IL).

Oxidative stress measurement

The protein concentration of extracts was assayed using a BCA assay kit from Bio-Rad Laboratories. Lipid peroxidation was evaluated by measuring the production of malondialdehyde (MDA) using a lipid peroxidation MDA assay kit (Beyotime, Shanghai, China). Catalase (CAT) activity was assayed as previously described. Glutathione (GSH) was determined by a spectrophotometric method using Ellman's reagent. Myeloperoxidase (MPO) activity in the supernatant was measured and calculated based on changes in absorbance (at 460 nm) resulting from the decomposition of H_2O_2 in the presence of *o*-dianisidine.

Mitochondrial dysfunction measurement

Mitochondrial respiratory complex activity was measured by high-resolution respirometry using Oxygraph-2K (Oroboros Instruments, Innsbruck, Austria) as we recently described [14]. An ATP-Luciferase-Based Bioluminescence Assay Kit (Sigma-Aldrich) was used to measure ATP levels in the brain tissue lysates. Luminescence was measured using a TD 20/20 luminometer (Turner Designs, Sunnyvale, CA).

Statistical analyses

Data are reported as the mean ± standard deviation when appropriate. Differences in mean among groups were evaluated by one-way analysis of variance. Bonferroni tests were used for pairwise comparisons. All analyses were conducted in SPSS 13.0 (SPSS Inc., Chicago, IL). Statistical significance was accepted at $P < 0.05$.

Results

Effect of CLP on Omi/HtrA2 expression and Omi/HtrA2 translocation from mitochondria to the cytosol in the hippocampus

To evaluate the localization of Omi/HtrA2, the hippocampus was stained with MitoTracker and immunolabeled with anti-Omi/HtrA2 and cytosolic and mitochondrial fractions were isolated. As illustrated in Fig. 1A, in the untreated sham-operated animals, Omi/HtrA2 was mostly located in the mitochondria, with low levels in the cytoplasm. After CLP treatment, the hippocampus exhibited a mild increase in Omi/HtrA2 expression and a significant increase in cytosolic Omi/HtrA2, whereas mitochondrial Omi/HtrA2 expression was reduced, indicating that CLP-induced oxidative stress resulted in the translocation of Omi/HtrA2 from the mitochondria to the cytosol. β-Actin and Cox IV were used as internal controls to verify equivalent cytosolic and mitochondrial protein loading, respectively (Fig. 1B).

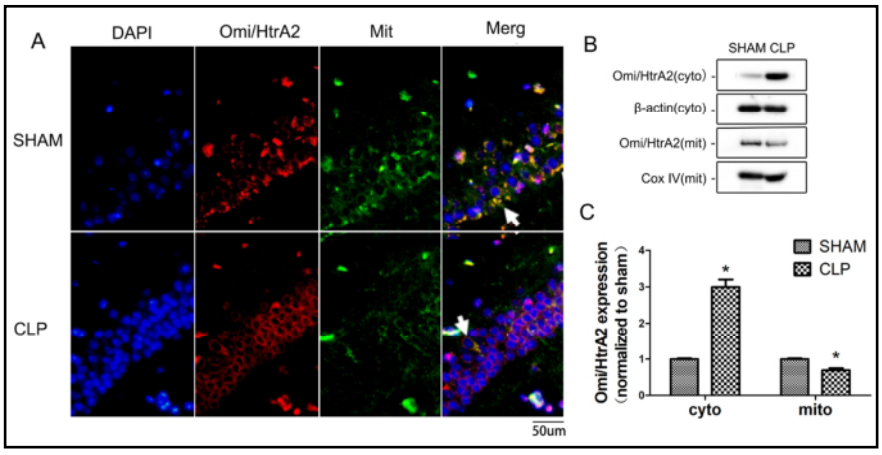

Fig. 1. Effect of CLP treatment on Omi/HtrA2 expression and Omi/HtrA2 translocation from mitochondria (mito.) to the cytosol (cyto.) in the hippocampus. (A) Co-localization of Omi/HtrA2 in mitochondria and the translocation of Omi/HtrA2 from the mitochondria to cytosol in hippocampal neurons, as determined by immunofluorescence. (B) Levels of Omi/HtrA2 were significantly decreased in the mitochondria and increased in the cytosol, as determined by western blotting. Respective bands with β-actin and COX IV as loading controls are shown. (C) Quantification of protein band density for mito. or cyto. relative to protein levels in untreated (SHAM) animals. *P<0.01 vs. SHAM group.

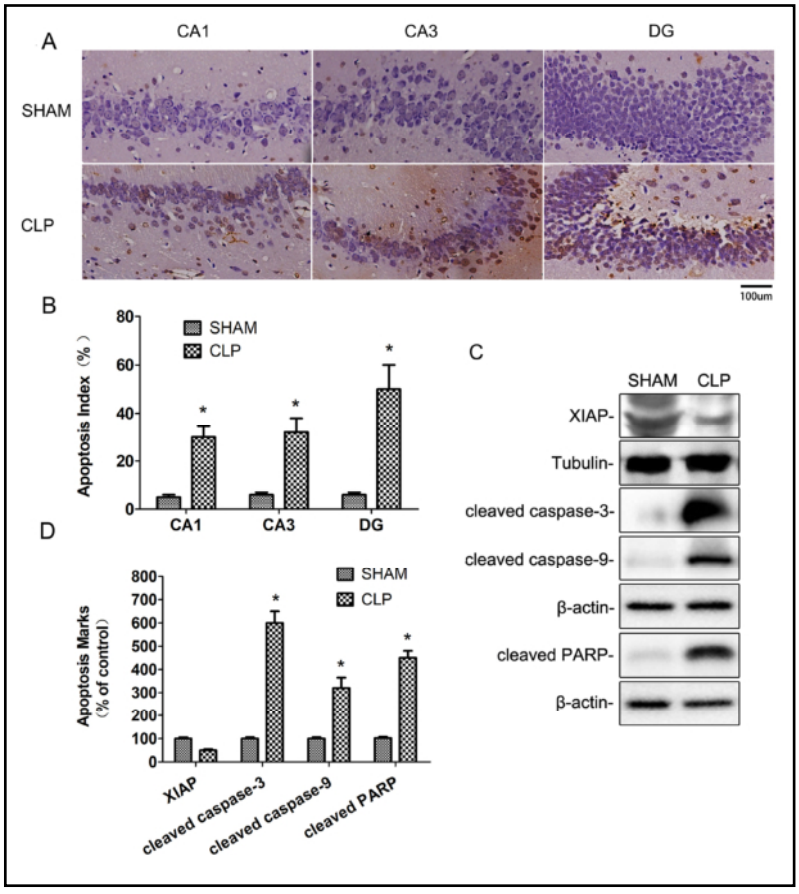

Fig. 2. Effect of CLP treatment on cell apoptosis and expression of the apoptosis inhibitor XIAP, caspases, and cleaved PARP in the hippocampus. (A) Cell apoptosis in hippocampal CA1, CA3, and dentate gyrus (DG) regions, as determined by TUNEL staining. (B) Quantitative analysis of TUNEL-positive cells of different groups. (C) Decreased level of XIAP and increased levels of cleaved caspase-3, cleaved caspase-9, and cleaved PARP in the hippocampus, as determined by western blotting. Respective bands with β-actin and Tubulin as loading controls are shown. (D) Quantification of protein band density was performed relative to protein levels in untreated (SHAM) animals. *P<0.01 vs. SHAM group.

Effect of CLP on apoptosis and the expression of the apoptosis inhibitor XIAP, caspases, and cleaved PARP in the hippocampus

As presented in Fig. 2A, few TUNEL-positive cells, indicating apoptosis, were detected in the untreated sham-operated animals. However, TUNEL-positive cells increased significantly 24 h after CLP. TUNEL-positive cells constituted up to 50.0% of the total cell population in the hippocampal dentate gyrus region (Fig. 2B).

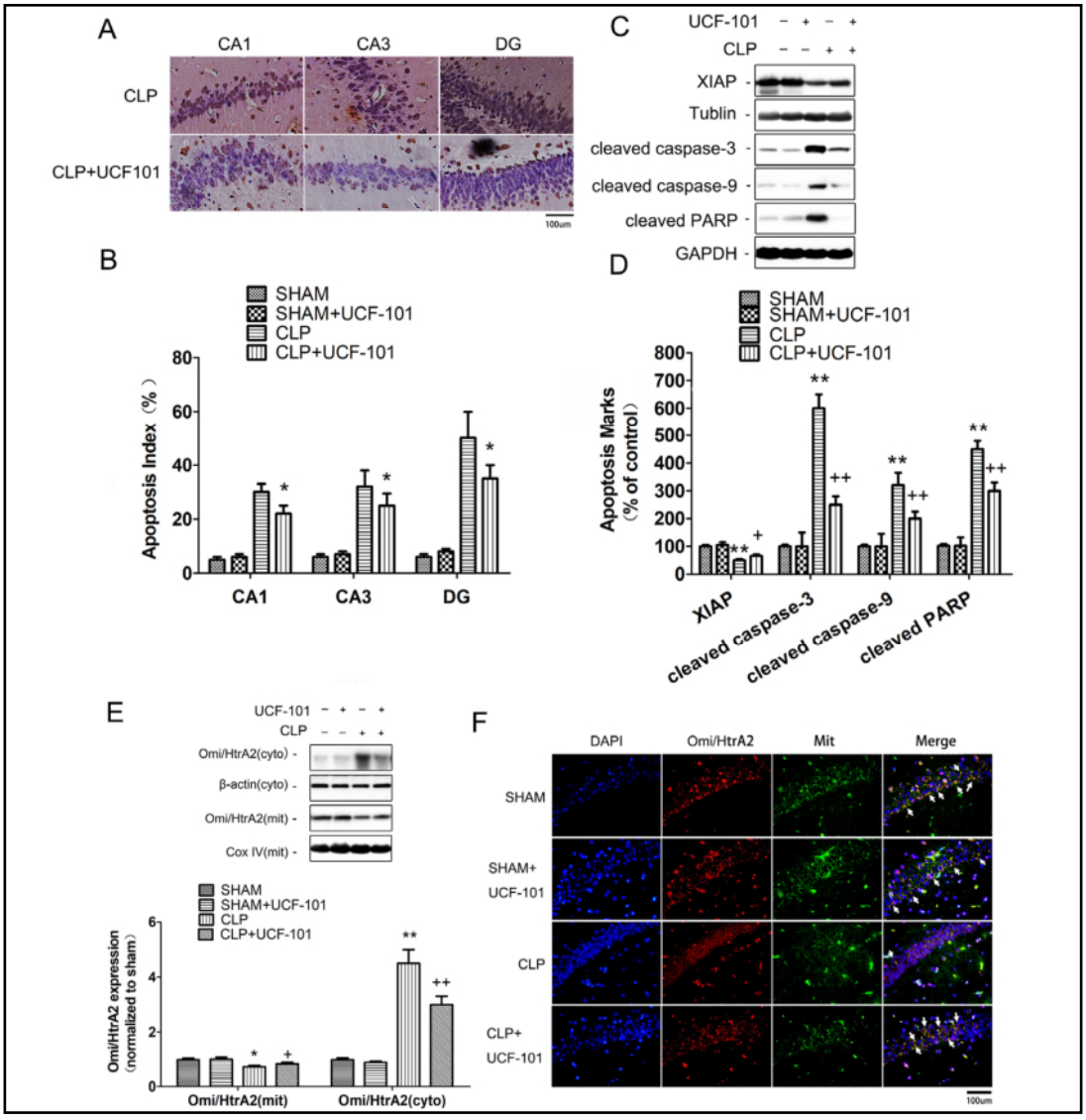

Fig. 3. Association of UCF-101 treatment with decreased cell apoptosis and Omi/HtrA2 translocation from the mitochondria to the cytosol in the hippocampus. (A) Cell apoptosis in hippocampal CA1, CA3, and dentate gyrus (DG) regions, as determined by TUNEL staining. (B) A quantitative analysis of TUNEL-positive cells in various groups. (C) Levels of XIAP, cleaved caspase-3, cleaved caspase-9, and cleaved PARP in the hippocampus, as determined by western blotting. Respective bands with GAPDH and Tubulin as loading controls are shown. (D) Quantification of protein band density was performed relative to protein levels in untreated (SHAM) animals. (E) Levels of Omi/HtrA2 in the mitochondria and cytosol, as determined by western blotting. Respective bands with β-actin and COX IV as loading controls are shown. Quantification of protein band density for mito. or cyto. relative to protein levels in untreated (SHAM) animals. (F) Co-localization of Omi/HtrA2 in mitochondria and translocation of Omi/HtrA2 from mitochondria to the cytosol in hippocampal neurons, as determined by immunofluorescence. *P<0.05 vs. SHAM group, **P<0.01 vs. SHAM group, ++P<0.01 vs. CLP group.

Prior studies have indicated that Omi/HtrA2 increases apoptosis via the proteolytic degradation of proteins that normally inhibit caspase activity. Omi/HtrA2 not only binds directly to X-linked inhibitor of apoptosis (XIAP) via its reaper motif but also results in XIAP degradation via its protease activity [7, 8]. XIAP levels in the hippocampus were significantly lower in the CLP group than in the sham-operated group, suggesting that XIAP degradation occurred after oxidative stress induced by CLP (Fig. 2C–D).

We further evaluated whether these proapoptotic events are associated with caspase activation. Hippocampal cleaved caspase-3, cleaved caspase-9, and cleaved PARP levels in animals subjected to CLP were significantly higher than those in sham-operated animals. These findings suggest that enhanced Omi/HtrA2 expression after CLP-induced oxidative stress results in the activation of caspase-dependent apoptotic pathways.

UCF-101 results in decreased cell apoptosis and Omi/HtrA2 translocation to the cytosol in the hippocampus

Our findings implied an association between Omi/HtrA2 activation and the proapoptotic state of hippocampal cells after CLP-induced oxidative stress. We evaluated whether Omi/HtrA2 inhibition by UCF-101 could protect the survival of hippocampal cells after CLP-induced oxidative stress. TUNEL detection indicated that cell apoptosis was significantly reduced in the UCF-101-treated group (Fig. 3A, B). Furthermore, a western blot analysis showed that UCF-101 treatment decreases XIAP degradation as well as cleaved caspase-3, cleaved caspase-9, and cleaved PARP (Fig. 3C, D).

Immunofluorescence indicated that CLP treatment resulted in the translocation of Omi/HtrA2 from the mitochondria to the cytosol (Fig. 3E, F). However, we also found that UCF-101 could partially prevent the mobilization of Omi/HtrA2 from the mitochondria to the cytosol. Accordingly, we evaluated markers related mitochondrial functions, such as mitochondrial complexes activity and ATP generation. CLP caused significant decreases in mitochondrial complex I, II, III, and IV respiration and reduced ATP (Fig. 4A–E). UCF-101 treatment reversed mitochondrial dysfunction to some extent.

Mitochondrial dysfunction is often associated with mitochondrial fusion–fission balance. We further confirmed this by examining Mfn2, a marker of cell mitochondrial fusion, and Drp1, a marker of cell mitochondrial division. Based on western blotting, after

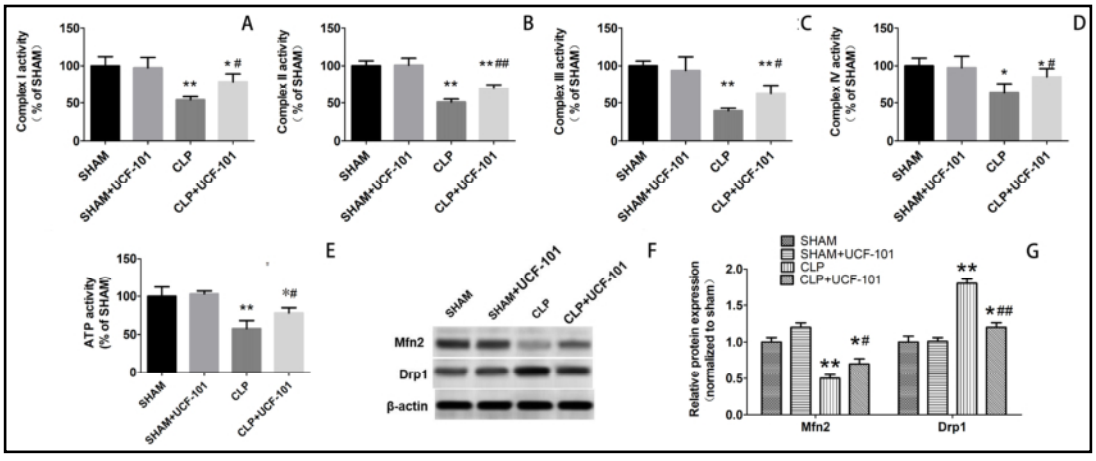

Fig. 4. Association of UCF-101 treatment with decreased mitochondrial dysfunction and mitochondrial fusion–fission balance. (A–D) Mitochondrial complex respiration. High-resolution respirometry was used to assess the status of mitochondrial complexes I, II, III, and IV. Values are oxygen flux expressed as a percentage of sham levels. (E) ATP levels are presented as percentages of sham levels. (F) Levels of Mfn2 and Drp1 in the hippocampus, as determined by western blotting. Respective bands with β-actin as loading controls are shown. (G) Quantification of protein band density was performed relative to β-actin.*P<0.05 vs. SHAM group, **P<0.01 vs. SHAM group, #P<0.05, vs. CLP group, ##P<0.01 vs. CLP group.

CLP treatment, hippocampal mitochondrial fusion decreased and fission increased. UCF-101 inhibited the down-regulation of Mfn2 and the up-regulation of Drp1 caused by CLP treatment, as indicated in Fig. 4F–G.

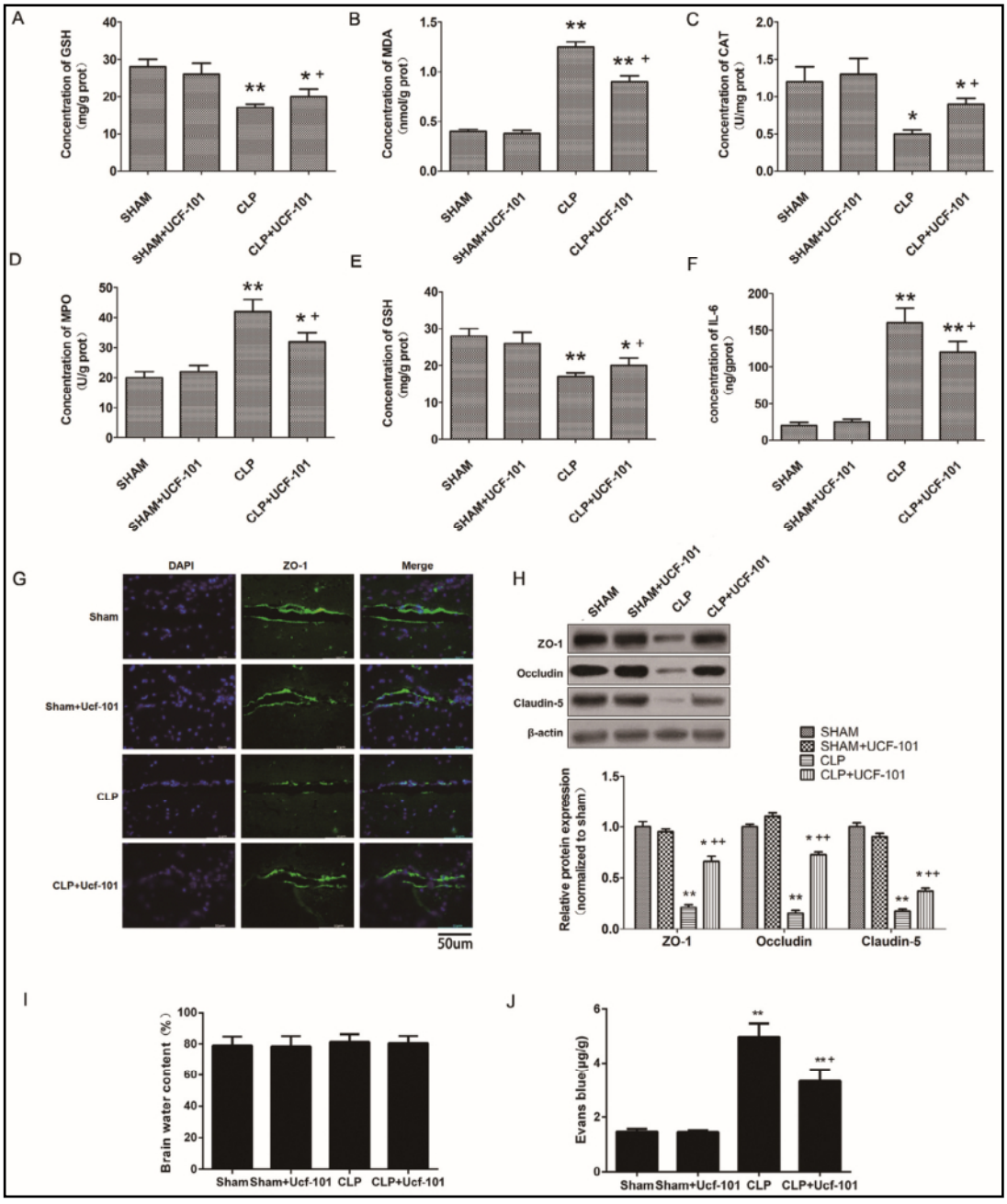

Fig. 5. Neuroprotective effects of UCF-101 in CLP-induced oxidative injury in hippocampus. (A–F) Effects of Omi/HtrA2 protease activity inhibition by UCF-101 on GSH, MDA, CAT, MPO, IL-6, and TNF-α levels in the hippocampus. (G) Effects of UCF-101 on brain tight junction protein ZO-1 expression in the hippocampus, as determined by immunofluorescence. (H) Effects of UCF-101 on occludin, claudin-5, and ZO-1 expression in the hippocampus, as determined by western blot analyses. Respective bands with β-actin as a loading control are shown at the bottom of the graphs. Quantification of protein band density was performed relative to protein levels in untreated (SHAM) animals.*P<0.05 vs. SHAM group, **P<0.01 vs. SHAM group. +P<0.05 vs. CLP group, ++P<0.01 vs. CLP group. (I) Effects of UCF-101 on brain edema, as determined by the wet/dry method. (J) Effects of UCF-101 on BBB permeability as determined by Evans blue extravasation.

Neuroprotective effects of UCF-101 in CLP-induced oxidative injury

The effects of Omi/HtrA2 inhibition by UCF-101 on oxidative stress and inflammation parameters, such as GSH, MDA, CAT, and MPO levels, are illustrated in Fig. 5A–F. The MDA concentration and MPO activity were significantly higher in the CLP-treated group than in the sham-operated group. However, the inhibition of Omi/HtrA2 by UCF-101 significantly decreased the MDA concentration and MPO activity. CAT and GSH levels were significantly lower in the CLP group than in the sham-operated group, and UCF-101 treatment significantly alleviated these effects of CLP. Compared with the sham-operated group, levels of the inflammatory cytokines interleukin (IL)-6 and tumor necrosis factor (TNF)-α were significantly higher in the CLP-treated group. However, UCF-101 resulted in the significant inhibition of IL-6 and TNF-α in the CLP+UCF-101 group compared with levels in the CLP group.

We further observed that the inhibition of Omi/HtrA2 by UCF-101 results in a significant improvement in the sepsis-induced loss of BBB integrity, as evidenced by an improvement in Evans blue extravasation (Fig. 5J). In line with the altered BBB permeability, we demonstrated the effects of the Omi/HtrA2 signaling pathway on BBB endothelial tight junction protein expression. As illustrated in Fig. 5G–H, western blot analyses and immunofluorescence indicated that Omi/HtrA2 inhibition abrogated the CLP-induced loss of occludin, claudin-5, and ZO-1 in the hippocampus. No significant effects of UCF-101 on brain edema were found using the wet/dry method.

Discussion

SAE is a diffuse brain dysfunction caused by sepsis. Its pathophysiological mechanism is complex and not fully resolved. It may involve brain microvascular endothelial cell dysfunction, destruction of the BBB, cerebral local inflammatory cell infiltration, inflammation medium, reduced cerebral perfusion, cerebral microvascular adjustment disorder, astrocyte and neuron dysfunction, neurotransmitter disorders, mitochondrial dysfunction, apoptosis, oxidative stress, calcium disorders, and so on [1, 13, 15]. Compelling evidence indicates that oxidative stress, mitochondrial dysfunction, and apoptosis play critical roles in the pathogenesis of SAE [16]. Accordingly, oxidative stress may promote the pathogenesis of SAE by enhancing the expression of proinflammatory cytokines, promoting apoptosis, and/or interfering with BBB function.

Mitochondria are major producers of ROS and the key organelle in apoptotic cell death [17]. Various pro-apoptotic stimuli increase outer mitochondrial membrane permeability, allowing the release of multiple mitochondrial pro-apoptotic proteins from the intermembrane space into the cytosol. Omi/HtrA2 is a proapoptotic protein that is released from mitochondria; it directly binds to XIAP and inhibits the caspase-inhibitory activity of XIAP [8]. In this study, we demonstrated the role of Omi/HtrA2 in hippocampus cell apoptosis in CLP-induced oxidative stress. Omi/HtrA2 regulates sepsis-induced cell apoptosis by translocation from mitochondria into the cytosol in the hippocampus and the subsequently induction of apoptosis. We also demonstrated that the inhibition of Omi/HtrA2 by the Omi/HtrA2 serine protease inhibitor UCF-101 partially reverses this apoptosis.

Omi/HtrA2 leads to apoptosis in hippocampal cells depending on protease activity and the caspase-mediated pathway. The degradation of the apoptotic inhibitory protein XIAP plays an important role. In this study, we showed that an increase in cytosolic Omi/HtrA2 after CLP treatment is correlated with a significant decrease in XIAP levels, presumably via Omi/HtrA2-mediated XIAP inhibition and degradation. Our results further show that significant XIAP degradation as well as significantly increased levels of cleaved caspase-3, cleaved caspase-9, and cleaved PARP in the septic hippocampus were markedly attenuated by UCF-101 treatment. These findings confirm that decreased inhibition of apoptosis by XIAP frees caspase-3 and caspase-9 to trigger the caspase-dependent apoptotic pathway.

Recent studies using *in vitro* and *in vivo* models have demonstrated that Omi/HtrA2 enhances apoptotic cell death by a postmitochondrial (inhibiting and or/degrading XIAP) mechanism, but not by a premitochondrial (enhancing mitochondrial permeability) mechanism [18-20]. These previous studies generally indicated that UCF-101 treatment only inhibits Omi/HtrA2 activation, but does not influence Omi/HtrA2 translocation from mitochondria to the cytosol. However, our results show that UCF-101 treatment decreases the translocation of Omi/HtrA2 from mitochondria to the cytosol after CLP treatment, which improves mitochondrial injury, as indicated by a better mitochondrial fusion–fission balance, decreased mitochondrial dysfunction, and the amelioration of oxidative stress. In line with our results, a previous *in vitro* study demonstrated that the extramitochondrial expression of Omi/HtrA2 indirectly induces the permeabilization of the outer mitochondrial membrane and subsequent Cyt c-dependent caspase activation in HeLa cells [21]. Their results indicated that the protease activity of Omi/HtrA2 promotes caspase activation via multiple pathways. Omi/HtrA2 can also induce apoptosis by degrading the apoptosis protein HAX-1 [22], mediating the p53 apoptosis pathway, and, indirectly, by enhancing the membrane permeability of the mitochondria.

Recent studies have illustrated the pathophysiology of SAE and encephalitis involving BBB dysfunction, neuroinflammation, and apoptosis [16, 23]. In this study, we observed that the inhibition of Omi/HtrA2 by UCF-101 substantially improves the sepsis-induced loss of BBB integrity, as demonstrated by improvements in Evans blue extravasation and endothelial tight junction protein expression. No significant effects of UCF-101 on brain edema were found. This suggests that Omi/HtrA2 protease-associated cell apoptosis may be involved in sepsis-induced BBB dysfunction and septic encephalopathy.

Conclusion

We demonstrated that Omi/HtrA2 regulates a mitochondria-dependent apoptotic pathway in a murine model of septic encephalopathy. We confirmed, for the first time, that *in vivo* oxidative stress promotes the mitochondria-to-cytosol translocation of Omi/HtrA2 in sepsis, leading to XIAP degradation, caspase activation, and subsequent apoptosis. The inhibition of Omi/HtrA2 by UCF-101 leads to neuroprotection by inhibiting the cytosolic translocation of Omi/HtrA2 and antagonizing the caspase-dependent apoptosis pathway. Therapeutic interventions that inhibit Omi/HtrA2 translocation or protease activity may provide a novel method to treat SAE.

Acknowledgements

This work was supported by the National Natural Science Foundation of China (Grant No. 81301610 and No.81100249). We also thank Dr. Cecilia He for her assistance with languge modification.

Disclosure Statement

No conflict of interests in this study.

References

1 Feng Q, Ai YH, Gong H, Wu L, Ai ML, Deng SY, Huang L, Peng QY, Zhang LN: Characterization of Sepsis and Sepsis-Associated Encephalopathy. J Intensive Care Med 2017;10.1177/0885066617719750885066617719750.

2 Ely EW, Shintani A, Truman B, Speroff T, Gordon SM, Jr HF, Inouye SK, Bernard GR, Dittus RS: Delirium as a predictor of mortality in mechanically ventilated patients in the intensive care unit. Jama 2004;291:1753.
3 Kinjo ER, Bozza FA, Cunha FQ, Castrofarianeto HC, D'Avila JC, Lopes LR, Britto LR, Hernandes MS, Reis PA, Trevelin SC: The role of Nox2-derived ROS in the development of cognitive impairment after sepsis. J Neuroinflammation 2014;11:36.
4 Berg RMG, Møller K, Bailey DM: Neuro-oxidative-nitrosative stress in sepsis. J Cereb Blood Flow Metab 2011;31:1532-1544.
5 Michels M, Vieira AS, Vuolo F, Zapelini HG, Mendonça B, Mina F, Dominguini D, Steckert A, Schuck PF, Quevedo J: The role of microglia activation in the development of sepsis-induced long-term cognitive impairment. Brain Behav Immun 2015;43:54-59.
6 Stepien KM, Heaton R, Rankin S, Murphy A, Bentley J, Sexton D, Hargreaves IP: Evidence of Oxidative Stress and Secondary Mitochondrial Dysfunction in Metabolic and Non-Metabolic Disorders. J Clin Med 2017;6:1-25.
7 Srinivasula SM, Gupta S, Datta P, Zhang Z, Hegde R, Cheong N, Fernandesalnemri T, Alnemri ES: Inhibitor of apoptosis proteins are substrates for the mitochondrial serine protease Omi/HtrA2. J Biol Chem 2003;278:31469.
8 Yang QH, Church-Hajduk R, Ren J, Newton ML, Du C: Omi/HtrA2 catalytic cleavage of inhibitor of apoptosis (IAP) irreversibly inactivates IAPs and facilitates caspase activity in apoptosis. Genes Dev 2003;17:1487-1496.
9 Hu Y, Huang M, Wang P, Xu Q, Zhang B: Ucf-101 protects against cerebral oxidative injury and cognitive impairment in septic rat. Int Immunopharmacol 2013;16:108-113.
10 Watson, Charles: The rat brain in stereotaxic coordinates, Academic Press 1986.
11 Chu K, Jeong SW, Jung KH, Han SY, Lee ST, Kim M, Roh JK: Celecoxib induces functional recovery after intracerebral hemorrhage with reduction of brain edema and perihematomal cell death. J Cereb Blood Flow Metab 2004;24:926-933.
12 Niu J, Hu R: Role of flunarizine hydrochloride in secondary brain injury following intracerebral hemorrhage in rats. Int J Immunopathol Pharmacol 2017;30:413-419.
13 Adam N, Kandelman S, Mantz J, Chrétien F, Sharshar T: Sepsis-induced brain dysfunction. Expert Rev Anti Infect Ther 2013;11:211-221.
14 Patil NK, Parajuli N, Macmillancrow LA, Mayeux PR: Inactivation of renal mitochondrial respiratory complexes and manganese superoxide dismutase during sepsis: mitochondria-targeted antioxidant mitigates injury. Am J Physiol Renal Physiol 2014;306:F734.
15 Dalpizzol F, Tomasi CD, Ritter C: Septic encephalopathy: does inflammation drive the brain crazy? Rev Bras Psiquiatr 2014;36:251-258.
16 Chaudhry N, Duggal AK: Sepsis Associated Encephalopathy. Adv Med 2014;2014:762320.
17 Mcmanus MJ, Murphy MP, Franklin JL: Mitochondria-derived reactive oxygen species mediate caspase-dependent and -independent neuronal deaths. Mol Cell Biol 2014;63:13-23.
18 Cilenti L, Lee Y, Hess S, Srinivasula S, Park KM, Junqueira D, Davis H, Bonventre JV, Alnemri ES, Zervos AS: Characterization of a novel and specific inhibitor for the pro-apoptotic protease Omi/HtrA2 J Biol Chem 2003;278:11489-11494.
19 Kim J, Kim DS, Park MJ, Cho HJ, Zervos AS, Bonventre JV, Park KM: Omi/HtrA2 protease is associated with tubular cell apoptosis and fibrosis induced by unilateral ureteral obstruction. Am J Physiol Renal Physiol 2010;298:1332-1340.
20 Liu HR, Gao E, Hu A, Tao L, Qu Y, Most P, Koch WJ, Christopher TA, Lopez BL, Alnemri ES: Role of Omi/HtrA2 in Apoptotic Cell Death After Myocardial Ischemia and Reperfusion. Circulation 2005;111:90.
21 Suzuki Y, Takahashi-Niki K, Akagi T, Hashikawa T, Takahashi R: Mitochondrial protease Omi/HtrA2 enhances caspase activation through multiple pathways. Cell Death Differ 2004;11:208.
22 Cilenti L, Soundarapandian MM, Kyriazis GA, Stratico V, Singh S, Gupta S, Bonventre JV, Alnemri ES, Zervos AS: Regulation of HAX-1 anti-apoptotic protein by Omi/HtrA2 protease during cell death. J Biol Chem 2004;279:50295-50301.
23 Varatharaj A, Galea I: The blood-brain barrier in systemic inflammation. Brain Behav Immun 2017;60:1-12.